



Removal of tetracycline using new biocomposites from aqueous solutions

Mehtap Erşan

Faculty of Engineering, Chemical Engineering Department, Cumhuriyet University, 58140 Sivas, Turkey, Tel. +90 5326680579; Fax: +90 3462191010; emails: mersan@cumhuriyet.edu.tr, gorgun7@hotmail.com

Received 20 January 2015; Accepted 18 March 2015

ABSTRACT

This study investigated the removal of tetracycline (TC) using polypropylene (PP), polystyrene (PS), *Saccharomyces cerevisiae* (Sc) yeast, and new types of sorbents such as polypropylene–*S. cerevisiae* (PP–Sc) and Polystyrene–*S. cerevisiae* (PS–Sc) biocomposites from aqueous solutions in a batch system. PP–Sc and PS–Sc are newly synthesized yeast immobilized polymers for the removal of TC. The experimental results showed that the maximum TC removal was obtained by using the PP–Sc biocomposite, which has a porous structure necessary for the adsorption process and live yeast is a good biosorbent that is necessary for the biosorption process. The experimental conditions were investigated as a function of pH (4–12), the TC amount (10–150 mg/L), the adsorbents amount (0.05–0.6 g/L), the temperature (25–55 °C), and the NaNO₃ amount (0.025–1 mg/L). The Freundlich and Langmuir adsorption isotherms were conducted to deduce the mechanism of the removal process and both of the results were compatible. The thermodynamic parameters for the removal process and the structure characteristics of PP–Sc, both before and after the TC removal, were determined. This study proved that the PP–Sc and PS–Sc biocomposites have different features than the original and can cause significant implications for environmental biotechnologies, in particular for the removal of TC.

Keywords: Tetracycline removal; Polypropylene–*Saccharomyces cerevisiae* biocomposite; Polystyrene–*Saccharomyces cerevisiae* biocomposite

1. Introduction

The pharmaceutical residues found in wastewater treatment plants are antibiotics, blood lipid regulators, antiinflammatories, antiepileptics, tranquillizers, X-ray contrast agents, and contraceptives. The removal of organic micropollutants in a wastewater unit processes is determined with different methods. Their biodegradability and physicochemical properties, their water solubility, hydrophobicity, and their tendency to volatilize are important parameters to determine the micropollutants [1]. Antibiotics are the drugs that are most used for preventing and treating human, animals,

and plants diseases [2]. These antibiotics can be divided into seven major categories: (1) aminoglycosides, (2) amphenicols, (3) β -lactams, (4) macrolides, (5) antibiotic peptides, (6) polyethers or ionophores, and (7) tetracyclines (TCs). TCs are one of the most widely used antibiotics in the world, which are poorly absorbed into the digestive tract, and are unchanged when excreted in feces and urine [3]. On account of a broad spectrum of antimicrobial activity, low cost, and wide applications of TC, this has led to concerns with regard to the unsafe residue which is toxic and can provoke allergies [4]. It also has the potential to promote or maintain bacterial

resistance and disrupt key cycles/processes that are critical to aquatic ecology or crop and animal production [5]. However, only a small portion of TC was metabolized or absorbed *in vivo*, while most of the unchanged forms were released in excreta [6]. TC is an amphoteric molecule ($C_{22}H_{24}N_2O_8$) and it has multiple ionizable functional groups of binding carbon atoms. These groups are tricarbonyl amide (C-1; C-2; C-3), phenolic diketone (C-10; C-11; C-12), and dimethylamine (C-4) groups (Fig. 1).

TC has three pK_a values (3.3, 7.68, and 9.69) and exists as a cationic, zwitterionic, and anionic species under acid, respectively. In aqueous solutions, the three groups can undergo protonation–deprotonation reactions and form cation species ($pH < 3.3$), zwitterion species ($3.3 < pH < 7.68$), or anion species ($pH > 7.68$) [7,8].

The adsorption into suspended solids, aerobic and anaerobic biodegradation, chemical (abiotic) degradation, and volatilization are the primary removal mechanisms for pharmaceutical residues in wastewater [1]. However, among these techniques, the adsorption of antibiotics by different sorbents is believed to be cheap and easy [9]. Iron oxide-coated quartz [10], marine sediments [11], rectorite [12], aluminum oxide [13], magnetite nanoparticles (Fe_3O_4 MNPs) [14], Fe–Mn binary oxide [15], palygorskite [16], inorganic graphene oxide [17], cinnamon soil [18], several soils [19], modified nanoscale zero valent iron [20], chitosan particles [21], and titania–silica composed materials [22] are widely used for the removal of TC.

Additionally, all of these sorbents, some algae species, polymers, and composite sorbents have been used for the removal of TC [23]. Unlike previous studies, this study used polypropylene (PP), polystyrene (PS), and *Saccharomyces cerevisiae* (*Sc*) to remove the TC. Polypropylene–*S. cerevisiae* (PP–*Sc*) and polystyrene–*S. cerevisiae* (PS–*Sc*) biocomposites were synthesized to evaluate the removal characteristics of TC on new immobilized materials. PP–*Sc* and PS–*Sc* biocomposites tend to be two inexpensive and widely available with

environmental impact on resistant polymers and yeast. PP is a non-toxicity polymer and the immobilization of *Sc* onto PP is a very hard process due to *Sc* being a micro-organism.

In this study, the immobilization process was performed and proved by an scanning electron microscope (SEM) and FTIR analysis. PP, PS, *Sc*, PP–*Sc*, and PS–*Sc* can accomplish the removal of a TC aqueous solution. Adsorption isotherms and thermodynamic parameters were represented. Functional groups and the PP–*Sc* morphology, which is the best adsorbent removal of TC in this study, were investigated with FTIR and SEM, both before and after the removal treatment.

2. Materials and methods

2.1. Materials

TC hydrochloride was purchased from Merck (Darmstadt, Germany) and was used to prepare a stock solution of 1,000 mg/L TC. The stock TC solution was diluted to different desired concentrations. The pH of the TC solution was adjusted to a required value using 0.1 M HCl and 0.1 M NaOH. *S. cerevisiae* (*Sc*), PP, and PS were obtained from Sigma.

2.2. Preparation of sorption material

Sc was dissolved into distilled water and 1,000 mg/L stock solutions were prepared at pH 9. PP and PS polymers added the desired amount to the solutions as a total 0.5 g weighing dry PP or PS polymers: 0.5 g weighing dry *Sc*. The mixture was shaken for 24 h and then the mixture was filtered. This mixture was dried in an oven at 30°C and a sorption material was obtained. Supernatant was collected to assess the amount of *Sc* released back into the washing solution.

2.3. Batch adsorption studies

The batch experiments were carried out in 100-mL PP bottles containing 100 mL of aqueous solution. For each experiment, 1 g of sorbent was added into 100 mL of TC solution in a 250-mL Erlenmeyer flask. The Erlenmeyer flasks were agitated in a shaker controlled at 100 rpm and at room conditions. 1 mol/L NaOH or 1 mol/L HCl were used to adjust the pH value. The concentrations of TC remained in their solution after the adsorption process and were measured using the UV spectrometer at 360 nm (Unicam UV 2). The absorbance values were taken against a blank solution (the blank solution was prepared by

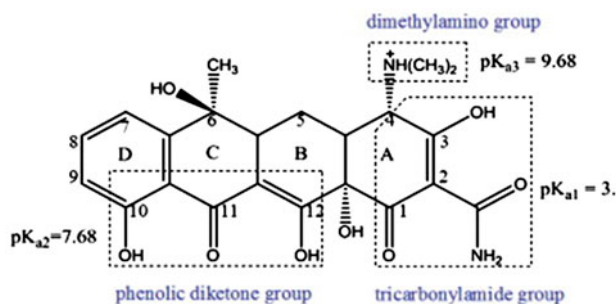


Fig. 1. Structure of tetracycline (TC) [8].

treating some amount of distilled water with sorbents at the same pH).

2.4. The equilibrium of mathematically

The removal yield was calculated as shown in Eqs. (1) and (2).

$$\text{Removal } \% = \frac{C_0 - C_t}{C_t} \times 100 \quad (1)$$

$$q_e = \frac{V(C_0 - C_t)}{m} \quad (2)$$

where q_e is the adsorption capacity (mg/g), C_0 and C_t are the initial and the after adsorption TC concentration (mg/L), V is the volume of the solution (L), and m is the amount of the sorbent (g).

2.5. Adsorption isotherms

Often these non-linear curves are called adsorption isotherms. Adsorption isotherms are mathematical models which describe the TC ions distribution between the solution and the adsorbent at a constant temperature, according to the equation. The Freundlich and Langmuir isotherms are defined for the most used one-component systems.

2.5.1. Langmuir adsorption isotherm

The Langmuir equation is valid for monolayer sorption onto a homogenous surface. It assumes that a reactive molecule is adsorbed on an active site, but also that further adsorption cannot take place at the same site [9]. The Langmuir adsorption isotherm can be written in linear form as follows:

$$\frac{1}{q_e} = \frac{1}{q_{\max}} + \frac{1}{C_e} \frac{1}{k_a q_{\max}} \quad (3)$$

where q_e (mg/g) is the equilibrium amount of the TC adsorbed per unit mass of sorbent values. Here, q_{\max} is the maximum TC adsorption capacity (mg/g), C_e is the equilibrium TC concentration in the liquid-phase concentration (mg/L), and k_a is the Langmuir adsorption constant (mg/L) [24].

2.5.2. Freundlich adsorption isotherm

The Freundlich adsorption isotherm can be written in the linear form as Eq. (4).

$$\ln q_e = \ln K_f + \frac{1}{n_f} \ln C_e \quad (4)$$

where K_f is the equilibrium constant and $1/n_f$ are the Freundlich constants that indicate the adsorption capacity and adsorption intensity, respectively. The Freundlich isotherm indicates the heterogeneous surface and this model better suited for the multilayer adsorption process [4].

2.6. Adsorption thermodynamics of TC

In this study, the thermodynamic parameters were investigated for the optimum experimental conditions. The free energy of adsorption (ΔG), the heat of adsorption (ΔH), and the entropy changes (ΔS) can be calculated from the following Eqs. (5) and (6) [25,26]:

$$K_d = \frac{q}{C_e} \quad (5)$$

$$\Delta G = -RT \ln K_d \quad (6)$$

where K_d is the equilibrium constant, ΔG is the free energy of adsorption (kJ/mol), T is the temperature in Kelvin, and R is the universal gas constant (8.314 J/mol K). Using Eq. (7), $\ln K_d$ is the value plotted against $1/T$ that is the value (Van't Hoff) consisting of the slope and the intercept, respectively, ΔS_0 , $-\Delta H_0$ [27].

$$\ln K_d = -\Delta H/RT + \Delta S/R \quad (7)$$

3. Results and discussion

3.1. Characterization of adsorbents (PP, PP-Sc, and PP-Sc after adsorption)

The SEM and FTIR patterns of PP and PP-Sc (before and after the treatment) are presented in Figs. 2 and 3, respectively. The SEM is a good method and widely used to investigate the morphological features of adsorbent materials. Fig. 2(a)–(c) shows the scanning of the electron microscopy images of PP, PP-Sc, and PP-Sc after the TC adsorption. Fig. 2(a) indicates a flat structure of PP changed after the synthesized PP-Sc biocomposite (Fig. 2(b)). A roughly flat-shaped PP turned into a spherical-shaped PP-Sc biocomposite, which is favorable for the adsorption of TC. The reason for that is the amorphous structure of Sc [28]. As a result, TC was adsorbed on the PP-Sc biocomposite surface (Fig. 2(c)).

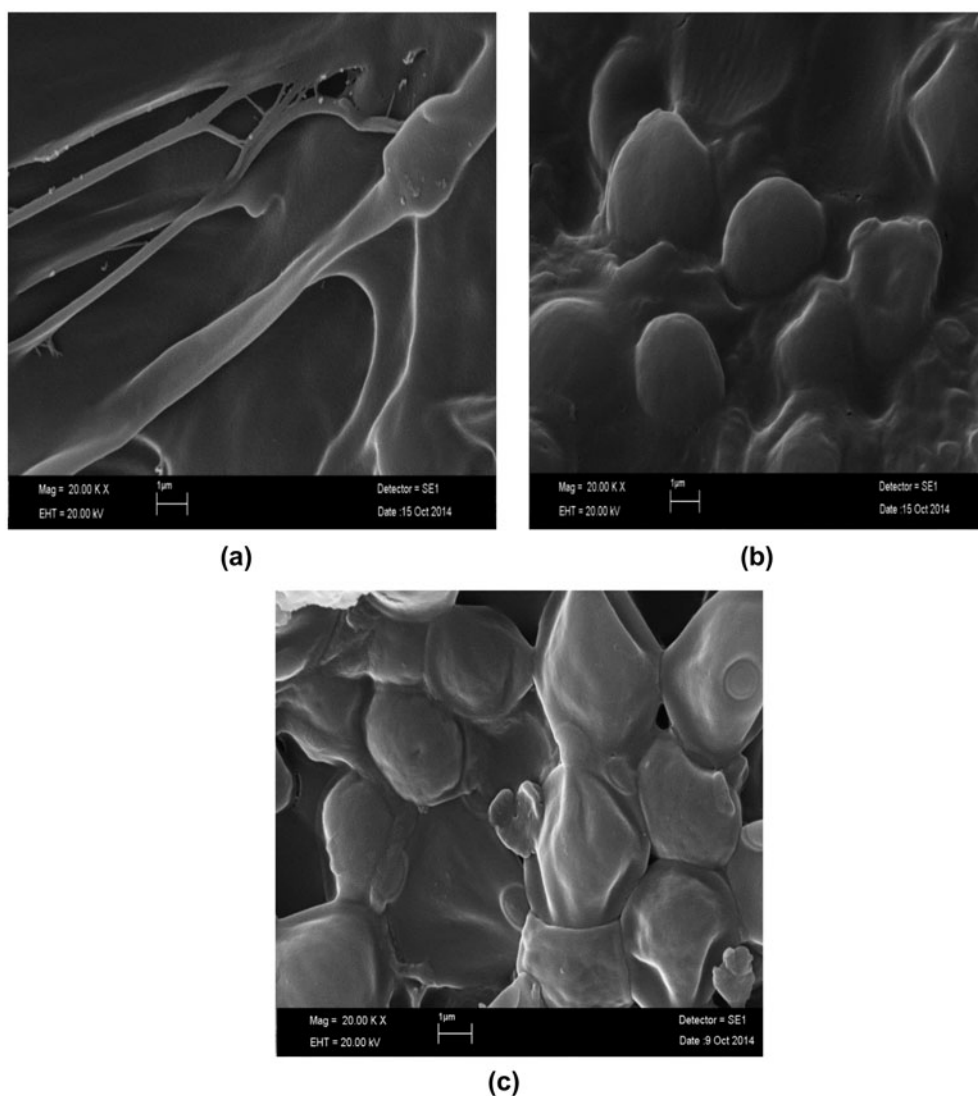


Fig. 2. (a) PP SEM images, (b) PP-Sc SEM images, and (c) PP-Sc SEM image after adsorption TC.

A FT-IR spectroscopy was used to determine the vibrational characteristics of chemical functional groups in the biosorbent [28,29]. The absorbance spectrums of PP, PP-Sc, and PP-Sc after the adsorption process were compared in order to determine the effects of Sc on PP and TC on PP-Sc. All of these pics were also displayed with the same graphic to compare them (Fig. 3(a)–(d)). A peak in the $1,300\text{--}400\text{ cm}^{-1}$ region shows the molecule structure. A number of inorganic groups such as sulfate, phosphate, nitrate, and carbonate absorbed in the fingerprint region ($<1,200\text{ cm}^{-1}$ or $8.3\text{ }\mu\text{m}$). The resulting spectra frequently exhibit bands at $3,450$ and $1,640\text{ cm}^{-1}$ due to the moisture absorbed [30]. Sc has various functional groups [31]. The two pics at about $1,345$ and $1,450\text{ cm}^{-1}$ are characteristic groups for C–H groups

(Fig. 3(a) and (b)). C–O–C stretching vibration at about $1,237.65\text{ cm}^{-1}$ for the PP-Sc biocomposite, but this peak cannot appear after the adsorption process (Fig. 3(c)). It shows that the TC molecules entering into the biocomposite molecules and changed the structure. A peak in the $3,500\text{--}3,200\text{ cm}^{-1}$ region is due to the stretching of the N–H bond of amino groups. This N–H stretching peak lies in the spectrum region occupied by a broad and strong band ($3,200\text{--}3,600\text{ cm}^{-1}$), which is due to the presence of $\gamma\text{O–H}$ of the hydroxyl groups [32]. The NH_2^+ , NH^+ , and N–H bond of biocomposites indicated peak lines in the $2,300\text{--}2,400\text{ cm}^{-1}$ region. The FTIR spectra of PP-Sc and PP-Sc-TC (before and after the adsorption of TC) appeared in protein-related bands, respectively, at $1,633.34$ and $1,634.37\text{ cm}^{-1}$. These bands indicated that

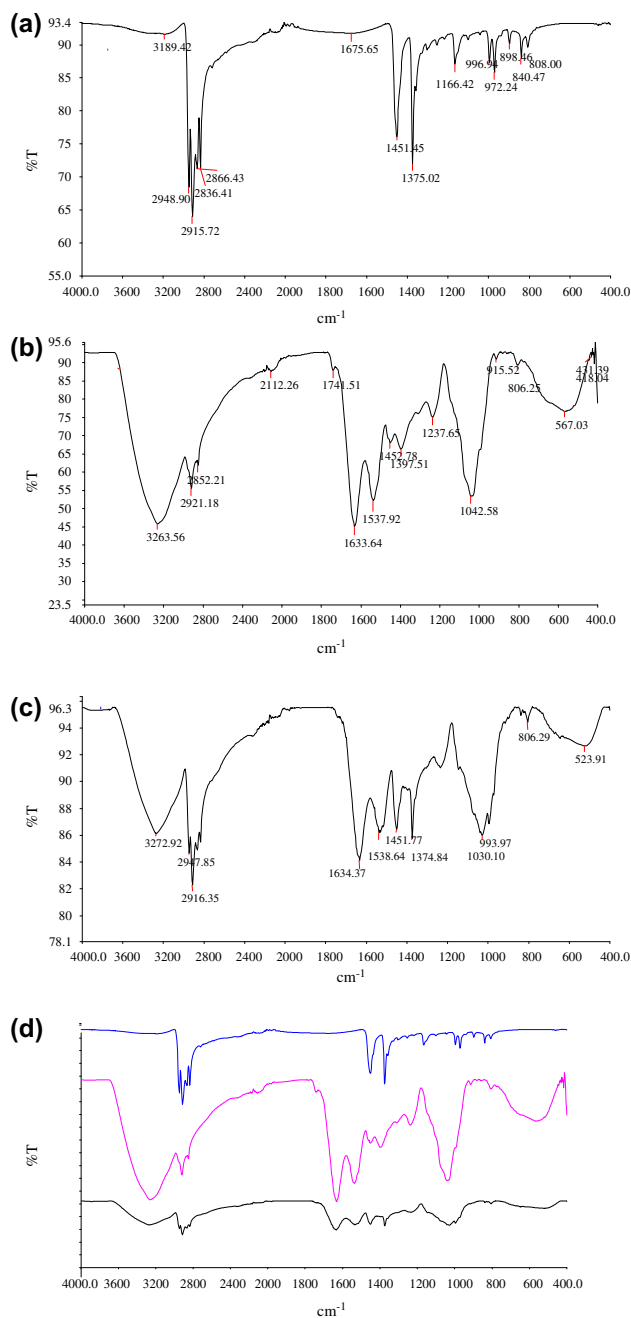


Fig. 3. (a) FTIR spectra of PP, (b) FTIR spectra of PP-Sc biocomposite, (c) FTIR spectra of PP-Sc biocomposite after TC sorption, and (d) FTIR spectra of PP, PP-Sc biocomposite, and PP-Sc biocomposite after TC sorption at the same graph.

a γ C_O of amide I and a H/ γ C_O combination of the amide II bonds. If there are carboxyl groups, the polysaccharide absorption peaks will appear between 1,000 and 1,100 cm^{-1} [33,34].

The PP-Sc and PP-Sc-TC carboxyl groups' bands appeared at 1,042.58 and 1,030.10 cm^{-1} , respectively.

The shifted bands show that the PP structure changed after the synthesized PP-Sc biocomposite and adsorption process. The reason for this may be due to the Sc's protein structure and the TC's amine and OH groups.

3.2. The effect of the pH

The pH value of the aqueous solution plays an important role in the adsorption and biosorption processes. It affects the speciation of TC, the surface characteristics of the biosorbent, and the chemical properties of the biosorbent during reaction [35, 36]. The effect of the initial pH on the TC removal at the range values 4–12 is presented in Fig. 4. Varying the initial pH value has an important effect on the efficiency of TC removal. The optimum removal efficiency was obtained at a pH of 6 and the value of the removal percentage of TC was decreased.

The effects of the pH on the TC removal process can explain with Sc, PP, and PS molecule structures and features. Sc is the most useful yeast for fermentation and it reproduces by a division process [37]. The solution charge is very important for the living media of Sc, the molecule strength of PP and PS, and the adsorption process because PP is a hydrophobic synthetic polymer [38] and PS can be soluble in organic solutions. The most important feature is Sc's outer layer of cell walls consisting of proteins which can be positively charged with ionizable groups of proteins in the TC media [39]. Therefore, the TC biosorption on Sc decreased after at pH 6 and the optimum pH value for TC biosorption was determined to be pH 6. There are some literature studies on the removal of different pollutants from aqueous solutions by PP, PS, their different composites, and a Sc immobilized polymer.

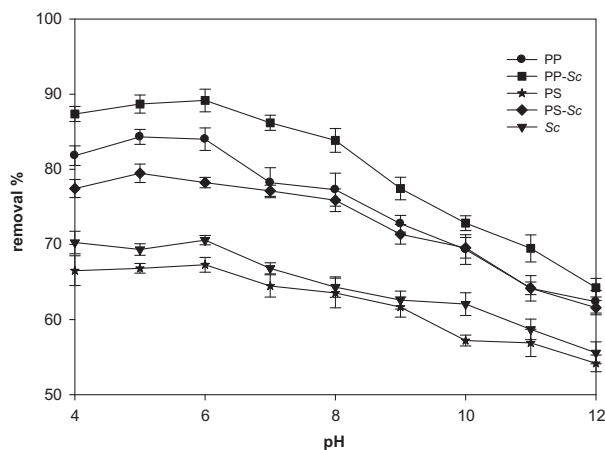


Fig. 4. The effect of pH of the solution on the removal of TC.

Motsa et al. [40] reported the application of clinoptilolite–polypropylene (CLI–PP) blends/composites for the removal of lead from aqueous media using a batch equilibrium adsorption method. The optimum pH was found to be between a pH of 6 and 8 [40]. In this study, the optimum pH for the removal of TC was found to be 6 and it is appropriate to range this in the literature as an immobilized *Sc*. Therefore, it can say that PP and PS do not affect structural properties of *Sc* in biocomposites, and biocomposites have gained outstanding features. PS has superior properties as well as PP. PS is an inexpensive plastic and may be easily recovered from waste. Presently, PS is widely used in many areas of biosciences and technologies owing to its simple preparation, ease of surface functionalization, and flexibility in size variations [41].

3.3. Effect of sorbent dosage

The effect of sorbent dosage on the TC adsorption was studied by varying the sorbent dose from 0.05 to 0.6 g and the results are presented in Fig. 5. In this study, four different sorbents were used. PP and PS are adsorbents used for the removal of TC, but *Sc* is a biosorbent. PP–*Sc* and PS–*Sc* combined both of these excellent features. It is clear that the removal of TC increased with the sorbent dosage. The removal of TC rapidly increased to 0.5 g per sorbent dosage then this increase slowly continued, but significant changes were not observed. The increase in the TC removal with an adsorbent dosage was due to an increase in the adsorptive and active sites of the adsorbent [42]. The optimum dosage of sorbents for further experiments of TC removal was found to be 0.05 g/L.

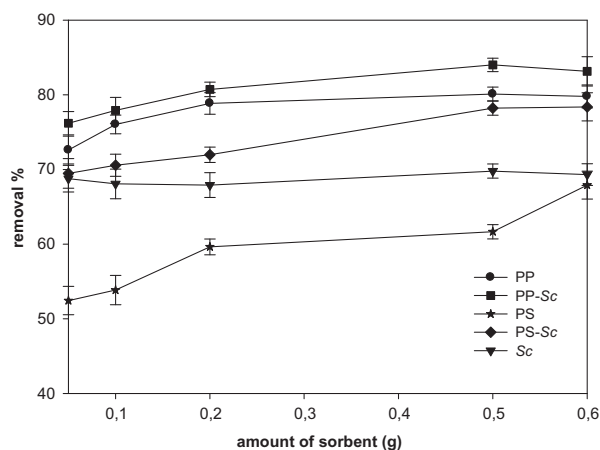


Fig. 5. The effect of sorbent dosage on the removal of TC.

3.4. Effect of time

The effect of the adsorption time on the TC adsorption was studied by varying the adsorption time from 2.5 to 240 min and the results are presented in Fig. 6. It is clear that the TC removal increased with the adsorption time (150 min), but a very long adsorption time causes desorption (240 min). Thus, the value of TC removal was decreased for four adsorbents and the optimum removal time was found to be 150 min.

Scientists investigated the removal time of TC by polymers and micro-organisms. de Godos et al. [23] investigated the mechanisms for the removal of TC in wastewater by high rate algal ponds. Dissolved TC removal was determined at $69 \pm 1\%$ and the scientists suggested that this removal was performed by photodegradation and biosorption from day 62 [23]. The removal of TC with sponge-like, tannin-based cryogels was investigated and the optimum removal time was found to be 150 min, similar to this study [4].

3.5. Effects of the initial TC amount

The effects of the initial TC amount on the removal of TC were studied by varying the TC amount (10–150 mg/L) and the results are presented in Fig. 7. The results show that by increasing the TC amount, it caused an increase in the removal of TC and the maximum q value was found to be 27.36 mg/g (PP).

3.6. Effect of cation

The effect of initial NaNO_3 amount on the removal of TC was studied by varying the NaNO_3 amount (0.025–1.0 mol/L) and the results are presented in

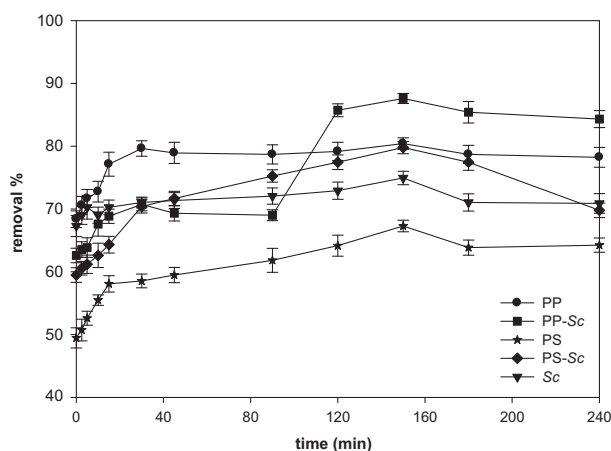


Fig. 6. The effect of time on the removal of TC (pH 6 $m_{\text{sorbent}} = 0.05$ g/L).

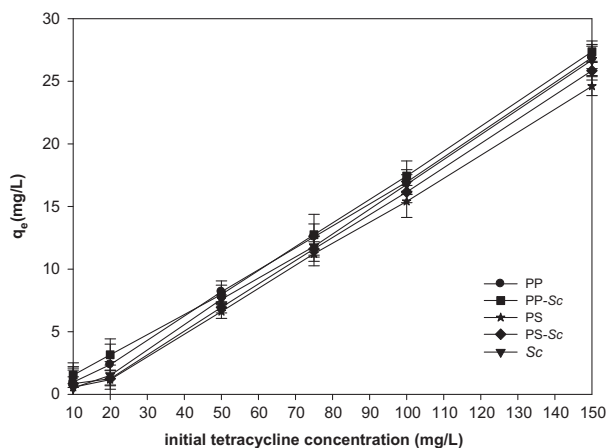


Fig. 7. The effects of the initial TC concentration on the removal of TC (pH 6, $m_{\text{sorbent}} = 0.05$ g/L).

Fig. 8. As seen in Fig. 8, the removal of TC by all of the sorbents decreased when increasing the ionic strength. These results can be explained by ionic and electrostatic forces of Na^+ and NO_3^- ions. The Na^+ ions compete with TC molecules for binding PP, PP + Sc, PS, PS + Sc, and Sc.

3.7. Determination of pH_{ZPC}

The zero point charge pH (pH_{ZPC}) of the adsorbents was measured for adsorbents. The pH_{ZPC} of the PP, PS, Sc, PP-Sc, and PS-Sc was determined by adding 20 mL of 0.05 mol/L NaCl to several 50-mL Erlenmeyer flasks. A range of initial pH (pH_i) values of the NaCl solutions was adjusted from 2 to 12. The suspensions were shaken in a shaker (298 K) for two days and suspensions were centrifuged (3,600 rpm, 15 min)

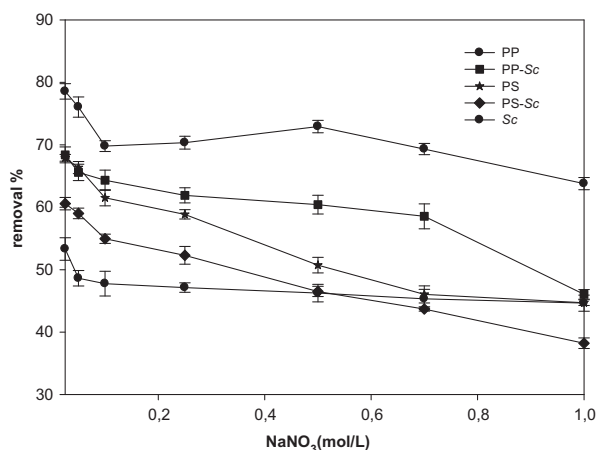


Fig. 8. The effect of NaNO_3 on the removal of TC (pH 6, $m_{\text{sorbent}} = 0.05$ g/L).

[43]. The value of pH_{ZPC} is the point where the curve of ΔpH ($\text{pH}_f - \text{pH}_i$) vs. pH_i crosses the line equal to zero [44]. The final pH (pH_f) values of the supernatant liquid were determined and the zero point charge results were shown in Table 1.

TC existed as cationic in strong acid solution at $\text{pH} < 3.3$, zwitter anions at $3.3 < \text{pH} < 7.7$, and negative ions at $\text{pH} > 7.7$ [45]. Optimum experimental pH value was determined as 6 and TC molecules have negative and positive charge at this pH. When pH of the solution increases above pH_{ZPC} , a negative charge is present on the surface of biocomposites [44]. The pH_{ZPC} of PP, PP-Sc, PS, PS-Sc, and Sc has shown that a negative charge at roughly $\text{pH} > 5.633$, 5.495, 5.595, 5.416, and 5.338, respectively. It causes better tetracycline cations adsorption through the electrostatic attraction phenomenon. It is shown that the main binding mechanism is due to the hydrogen bonding between the adsorbents and TC's $-\text{OH}$ group adjacent to tertiary amine $-\text{N}(\text{CH}_3)_2$ and electrostatic interaction may be the most probable bonding mechanism which is between protonated amine group of TC and the positively charged adsorbent wall [9]. At the same time, the adsorption mechanism of the negatively charged TC molecules occurs partly by ion exchange via releasing exchangeable proton, which is interactions between a adsorbed cation and a neutralized site [46,48].

3.8. Determination of adsorption isotherms

The value of R_L indicates the type of the isotherm to be irreversibly ($R_L = 0$), favorable ($0 < R_L < 1$), linear ($R_L = 1$), or unfavorable ($R_L > 1$).

The TC adsorption fits excellently with both Langmuir and Freundlich isotherms for PP, PP-Sc, PS, PS-Sc, and Sc. All isotherm graphs were plotted using Sigmaplot 11 software [45]. The applicability of both Langmuir and Freundlich isotherms on the adsorption of TC into biosorbent shows that the adsorption occurred at both specific localized sites on a homogeneous surface by the monolayer formation of an adsorbate onto: firstly, the adsorbent surface; and secondly, the reversible heterogeneous surface consisting of different adsorption energies at the adsorption sites [42].

Table 1
Zero point charge values of adsorbents

	pH_{ZPC}	r^2
PP	5.633	0.915
PP-Sc	5.495	0.9458
PS	5.595	0.9555
PS-Sc	5.416	0.9415
Sc	5.338	0.9191

Table 2 shows that adsorbents had an adsorption capacity. The adsorption capacity of some adsorbents was found to be graphene oxide functionalized magnetic particles of 39.1 mg/g [48] and anaerobic granular sludge of 4.61 mg/g [49], as found in the literature. In this study, the best adsorption capacity was found to be PP + Sc (18.346 mg/g) > PP + Sc (16.346 mg/g) > Sc (14.830 mg/g) > PP (12.723 mg/g) > PS (11.240 mg/g), respectively. The Langmuir isotherm is suitable for adsorbents data. These results are suitable and better than many studies found in the literature.

3.9. Determining of thermodynamic parameters

The 1/n heterogeneity values for magnetic biosorbent were between 0 and 1, indicating that the TC adsorption was favorable at the conditions studied. The calculated R_L values range between 0 and 1, indicating that the TC adsorption into a sorbent is favorable and suitable [28]. The thermodynamic parameters, Gibbs free energy (ΔG), entropy (ΔS), and enthalpy (ΔH) values are presented in Table 3. ΔG values presented for PP, PP-Sc, PS, and Sc at four temperatures. For the adsorption of TC on all of these adsorbents, ΔG values are negative and fairly close. The positive value of ΔS shows the increase in randomness at the solid/liquid interface during the adsorption process [50]. The adsorption of TC processes has negative ΔH values for four adsorbents. So that these adsorption processes are spontaneous and feasible. The enthalpy value for physical sorption is usually no more than 4.2 kJ/mol and the enthalpy for chemical sorption is more than 21 kJ/mol because chemical sorption involves forces much stronger than in physical sorption [43]. The enthalpy values were obtained for adsorbents and biosorbents were indicated the physical sorption process.

3.10. Kinetics of TC adsorption onto adsorbents

The effect of contact time in the range of 2.5–150 min and kinetics were calculated (pH 6,

Table 2
Langmuir and Freundlich isotherm parameters of the TC adsorption

	Langmuir			Freundlich		
	Q_{max} (mg/g)	b	r^2	K_f	$1/n_f$	r^2
PP	12.723	0.0527	0.944	2.737	0.554	0.983
PP-Sc	18.346	0.0391	0.955	1.844	0.465	0.908
PS	11.240	0.0372	0.929	3.4681	0.869	0.899
PS-Sc	16.343	0.0683	0.952	3.356	0.728	0.918
Sc	14.830	0.0654	0.922	3.423	0.900	0.907

Table 3
Thermodynamic parameters of the TC adsorption

T (°K)	PP	PP-Sc	PS	PS-Sc	Sc
ΔG (kJ/mol)					
298.15	-1.3448	-1.4184	-1.2690	-1.0498	-1.1441
308.15	-1.3040	-1.3725	-1.1793	-1.0031	-1.1693
318.15	-1.2975	-1.3642	-1.2549	-1.0029	-1.0932
328.15	-1.2223	-1.3614	-1.1324	-1.0005	-1.0484
ΔS (J/mol K)					
298.15	0.651	0.2283	0.8349	0.8021	0.4571
ΔH (kJ/mol)					
298.15	-1.4249	-1.6332	-2.0249	-3.0326	-2.0249

0.05 g/L TC). In order to investigate the mechanism of TC removal (adsorption and biosorption) by PP, PS, Sc, PP-Sc, and PS-Sc, the pseudo-first-order Lagergren, pseudo-second-order model, and intraparticle diffusion kinetic models were analyzed. The kinetic of TC removal by adsorbents and biocomposites was analyzed using the pseudo-first-order Lagergren, pseudo-second-order model, and intraparticle diffusion model.

The pseudo-first-order kinetic model is expressed as [51]:

$$\log(q_e - q_t) = \log q_e - \frac{k_1}{2.303} t \tag{8}$$

The pseudo-second-order kinetic model is given as [52]:

$$\frac{t}{q_t} = \frac{1}{k_2(q_e)^2} + \frac{t}{q_e} \tag{9}$$

The initial sorption rate h (mg/g min):

$$h = k_2 q_e^2 \tag{10}$$

Intraparticle diffusion model plays an important role in the extent of adsorption and the equation can be described as [53]:

$$q_t = k_d t^{0.5} + I \tag{11}$$

where q_e and q_t (mg/g) are the amounts of TC ions adsorbed on the adsorbent at equilibrium and time t (min), I is the intercept, and k_1 (min^{-1}), k_2 (g/mg min), and k_d ($\text{mg/g min}^{0.5}$) are the rate constants of pseudo-first-order kinetic model, pseudo-second-order kinetic

Table 4
Kinetic parameters of the TC adsorption

	Pseudo-first-order			Pseudo-second-order		
	$q_{e,exp}$	r^2	k_1 (min^{-1})	$q_{e,cal}$	r^2	k_2 ($\text{g}/\text{mg min}$)
PP	1.12	0.963	0.018	7.93	0.999	0.126
PP-Sc	1.78	0.963	0.021	8.76	0.999	0.061
PS	1.95	0.999	0.018	7.95	0.999	0.05
PS-Sc	2.07	0.967	0.019	6.43	0.997	0.045
Sc	4.38	0.962	0.025	7.01	0.999	0.073
Intraparticle						
						C
PP	$q_{e,cal}$ 6.945	r^2 0.969	k_a ($\text{mg}/\text{g min}^{0.5}$) 0.09			0.935
PP-Sc	6.773	0.922	0.174			1.253
PS	5.828	0.974	0.179			0.874
PS-Sc	4.115	0.922	0.198			1.254
Sc	6.739	0.956	0.021			2.457
h ($\text{mg}/\text{g min}$)						
PP	PP-Sc	PS	PS-Sc	Sc		
0.875	2.798	1.698	1.528	3.315		

model, and intraparticle diffusion model, respectively [45]. The values of correlation coefficients (k_1 , k_2 , k_d), equilibrium adsorption capacities ($q_{e,teo}$) in these models, and initial sorption rate (h) are given in Table 4.

According to the fitted linear regression plots, the experimental data are well fitted with the pseudo-second-order kinetic model with the highest value of correlation coefficients for PP, PP-*Sc*, PS, PS-*Sc*, and *Sc* ($R^2 > 0.999$). Kinetics of TC adsorption on PP, PP-*Sc*, PS, PS-*Sc*, and *Sc* followed the pseudo-second-order model. It is suggesting that the adsorption rate-limiting step may be the chemisorptions of TC. These mechanisms can occur via surface complexation reactions at specific adsorption sites [45,46]. In addition, in this present study, the plots indicated that the intraparticle diffusion model was not the sole rate-controlling step because it does not intersect at the origin. The “ C ” values of adsorbents are not equal the zero ($C \neq 0$) and *Sc* has the biggest “ C ” value (2.457). Therefore, both intraparticle diffusion and boundary diffusion highly affected the TC adsorption on PP-*Sc* and PS-*Sc* biocomposites than PP and PS.

4. Conclusion

In this research, the sorption of (TC) on PP, PS, *S. cerevisiae* (*Sc*) yeast, and new types of sorbents such as polypropylene-*S. cerevisiae* (PP-*Sc*) and polystyrene-*S. cerevisiae* (PS-*Sc*) was investigated. The results showed that the removal processes were relatively fast and reached equilibrium within 150 min. The pH of the solution and ionic strength had significant effects on the TC sorption for both types of sorbents. The negative values of ΔH , ΔG , and ΔS verify the exothermic and spontaneous nature of the removal process. FTIR and SEM analysis proved that polypropylene-*S. cerevisiae* (PP-*Sc*) and polystyrene-*S. cerevisiae* (PS-*Sc*) biocomposites have different features than PP, PS, and *Sc*, that is to say, their adsorption abilities increased. Therefore, these biocomposites can be used for an effective TC removal and have a high economic value as synthesized from a waste polymer.

References

- J.E. Drewes, Removal of pharmaceutical residues during wastewater treatment, in: M. Petrovic, D. Barcelo (Eds.), Analysis, Fate and Removal of Pharmaceuticals in the Water Cycle, vol. 50, Wilson & Wilson's, Elsevier, Amsterdam, 2007, pp. 427–447.
- J.L. Martinez, Environmental pollution by antibiotics and by antibiotic resistance determinants, Environ. Pollut. 157 (2009) 2893–2902.
- A.K. Sarmah, M.T. Meyer, A.B.A. Boxall, A global perspective on the use, sales, exposure pathways, occurrence, fate and effects of veterinary antibiotics (VAs) in the environment, Chemosphere 65 (2006) 725–759.
- M. Erşan, E. Bağda, E. Bağda, Investigation of kinetic and thermodynamic characteristics of removal of tetracycline with sponge like, tannin based cryogels, Colloids Surf., B 104 (2013) 75–82.
- A.J. Watkinson, E.J. Murby, S.D. Costanzo, Removal of antibiotics in conventional and advanced wastewater treatment: Implications for environmental discharge and wastewater recycling, Water Res. 41 (2007) 4164–4176.
- J.P. Bound, N. Voulvoulis, Pharmaceuticals in the aquatic environment—A comparison of risk assessment strategies, Chemosphere 56 (2004) 1143–1155.
- M.E. Parolo, M.C. Savini, J.M. Vallés, M.T. Baschini, M.J. Avena, Tetracycline adsorption on montmorillonite: pH and ionic strength effects, Appl. Clay Sci. 40 (2008) 179–186.
- Y. Zhao, Y. Tan, Y. Guo, X. Gu, X. Wang, Y. Zhang, Interactions of tetracycline with Cd (II), Cu (II) and Pb (II) and their cosorption behavior in soils, Environ. Pollut. 180 (2013) 206–213.
- E. Bağda, M. Erşan, E. Bağda, Investigation of adsorptive removal of tetracycline with sponge like, *Rosa canina* gall extract modified, polyacrylamide cryogels, J. Environ. Chem. Eng. 1 (2013) 1079–1084.
- E. Tanis, K. Hanna, E. Emmanuel, Experimental and modeling studies of sorption of tetracycline onto iron oxides-coated quartz, Colloids Surf., A 327 (2008) 57–63.
- X.R. Xu, X.Y. Li, Sorption and desorption of antibiotic tetracycline on marine sediments, Chemosphere 78 (2010) 430–436.
- P.H. Chang, J.S. Jean, W.T. Jiang, Z.H. Li, Mechanism of tetracycline sorption on rectorite, Colloids Surf., A 339 (2009) 94–99.
- W.R. Chen, C.H. Huang, Adsorption and transformation of tetracycline antibiotics with aluminum oxide, Chemosphere 79 (2010) 779–785.
- D. Zhang, H. Niu, X. Zhang, Z. Meng, Y. Cai, Strong adsorption of chlorotetracycline on magnetite nanoparticles, J. Hazard. Mater. 192 (2011) 1088–1093.
- H. Liu, Y. Yang, J. Kang, M. Fan, J. Qu, Removal of tetracycline from water by Fe–Mn binary oxide, Environ. Sci. 24 (2012) 242–247.
- P. Chang, Z. Li, T. Yu, S. Munkhbayer, T. Kuo, Y. Hung, J. Jean, K. Lin, Sorptive removal of tetracycline from water by palygorskite, J. Hazard. Mater. 165 (2009) 148–155.
- Y. Gao, Y. Li, L. Zhang, H. Huang, J. Hu, S.M. Shah, X. Su, Adsorption and removal of tetracycline antibiotics from aqueous solution by graphene oxide, J. Colloid Interface Sci. 368 (2012) 540–546.
- Y. Wan, Y. Bao, Q. Zhou, Simultaneous adsorption and desorption of cadmium and tetracycline on cinnamon soil, Chemosphere 80 (2010) 807–812.
- S.A. Sassman, L.S. Lee, Sorption of three tetracyclines by several soils: Assessing the role of pH and cation exchange, Environ. Sci. Technol. 39 (2005) 7452–7459.
- H. Chen, H. Luo, Y. Lan, T. Dong, B. Hu, Y. Wang, Removal of tetracycline from aqueous solutions using polyvinylpyrrolidone (PVP-K30) modified nanoscale zero valent iron, J. Hazard. Mater. 192 (2011) 44–53.
- A.L.P.F. Caroni, C.R.M. de Lima, M.R. Pereira, J.L.C. Fonseca, The kinetics of adsorption of tetracycline on

- chitosan particles, *J. Colloid Interface Sci.* 340 (2009) 182–191.
- [22] M. Brigante, P.C. Schulz, Removal of the antibiotic tetracycline by titania and titania–silica composed materials, *J. Hazard. Mater.* 192 (2011) 1597–1608.
- [23] I. de Godos, R. Muñoz, B. Guieysse, Tetracycline removal during wastewater treatment in high-rate algal ponds, *J. Hazard. Mater.* 229–230 (2012) 446–449.
- [24] I. Langmuir, The constitution and fundamental properties of solids and liquids, *J. Am. Chem. Soc.* 38 (1916) 2221–2295.
- [25] Y.S. Ho, Removal of copper ions from aqueous solution by tree fern, *Water Res.* 37 (2003) 2323–2330.
- [26] B. Zhu, Q. Feng, Q. Wang, T. Duan, L. Ou, G. Zhang, Y. Lu, Adsorption of Cu(II) ions from aqueous solutions on modified chrysotile: Thermodynamic and kinetic studies, *Appl. Clay Sci.* 80–81 (2013) 38–45.
- [27] E.W. Meijer, Jacobus Henricus van't Hoff; hundred years of impact on stereochemistry in the Netherlands, *Angew. Chem. Int. Ed.* 40 (2001) 3783–3789.
- [28] U.A. Guler, M. Sarioglu, Mono and binary component biosorption of Cu(II), Ni(II), and Methylene Blue onto raw and pretreated, *S. cerevisiae*: Equilibrium and kinetics, *Desalin. Water Treat.* 52 (2013) 1–18.
- [29] M. Mansal, U. Garg, D. Singh, V.K. Garg, Removal of Cr(VI) from aqueous solutions using pre-consumer processing agricultural waste: A case study of rice husk, *J. Hazard. Mater.* 162 (2006) 312–320.
- [30] D.A. Skoog, J.J. Leary, Principles of Instrumental Analysis, fourth ed., Saunders College Publishing Co., New York, NY, 1992.
- [31] J.K. Yu, M. Tong, X.M. Sun, B.H. Li, Enhanced and selective adsorption of Pb(II) and Cu(II) by EDTA-modified biomass of baker's yeast, *Bioresour. Technol.* 99 (2009) 2588–2593.
- [32] F. Pagnanelli, M. Petrangeli Papini, M. Trifoni, F. Vegliò, L. Toro, Biosorption of metal ions on *Arthrobacter* sp.: Biomass characterization and biosorption modeling, *Environ. Sci. Technol.* 34 (2000) 2773–2778.
- [33] S.K. Kazy, P. Sar, S.P. Singh, Asish K. Sen, S.F. D'Souza, Extracellular polysaccharides of a copper-sensitive and a copper-resistant *Pseudomonas aeruginosa* strain: Synthesis, chemical nature and copper binding, *World J. Microbiol. Biotechnol.* 18 (2002) 583–588.
- [34] S. Aytas, D.A. Turkozu, C. Gok, Biosorption of uranium(VI) by bi-functionalized low cost biocomposite adsorbent, *Desalination* 280 (2011) 354–362.
- [35] Q. Peng, Y. Liu, G. Zeng, W. Xu, C. Yang, J. Zhang, Biosorption of copper(II) by immobilizing *Saccharomyces cerevisiae* on the surface of chitosan-coated magnetic nanoparticles from aqueous solution, *J. Hazard. Mater.* 177 (2010) 676–682.
- [36] S.M. Nomanbhay, K. Palanisamy, Removal of heavy metal from industrial wastewater using chitosan coated oil palm shell charcoal, *Electron. J. Biotechnol.* 8 (2005) 43–53.
- [37] H. Feldmann, Horst Yeast, Molecular and Cell Bio, Wiley-Blackwell, Germany, 2010.
- [38] A. Boger, B. Heise, C. Troll, O. Marti, B. Rieger, Mechanical and temperature dependant properties, structure and phase transitions of elastic polypropylenes, *Eur. Polym. J.* 43 (2007) 634–643.
- [39] N.S. Maurya, A.K. Mittal, P. Cornel, E. Rother, Biosorption of dyes using dead macro fungi: Effect of dye structure, ionic strength and pH, *Bioresour. Technol.* 97 (2006) 512–521.
- [40] M.M. Motsa, J.M. Thwala, T.A.M. Msagati, B.B. Mamba, The potential of melt-mixed polypropylene–zeolite blends in the removal of heavy metals from aqueous media, *Phys. Chem. Earth* 36 (2011) 1178–1188.
- [41] K. Kim, H.B. Lee, H.K. Park, K.S. Shin, Easy deposition of Ag onto polystyrene beads for developing surface-enhanced-Raman-scattering-based molecular sensors, *J. Colloid Interface Sci.* 318 (2008) 195–201.
- [42] Z. Chen, T. Wang, X. Jin, Z. Chen, M. Megharaj, R. Naidu, Multifunctional kaolinite-supported nanoscale zero-valent iron used for the adsorption and degradation of crystal violet in aqueous solution, *J. Colloid Interface Sci.* 398 (2013) 59–66.
- [43] M. El Haddad, A. Regti, M.R. Laamari, R. Slimani, R. Mamouni, S.E. Antri, S. Lazar, Calcined mussel shells as a new and eco-friendly biosorbent to remove textile dyes from aqueous solutions, *J. Taiwan Inst. Chem. Eng.* 45 (2014) 533–540.
- [44] M. El Haddad, R. Mamouni, N. Saffaj, S. Lazar, Removal of a cationic dye — Basic Red 12 — from aqueous solution by adsorption onto animal bone meal, *J. Assoc. Arab Univ. Basic Appl. Sci.* 12 (2012) 48–54.
- [45] U.A. Guler, M. Sarioglu, Removal of tetracycline from wastewater using pumice stone: Equilibrium, kinetic and thermodynamic studies, *J. Environ. Health Sci. Eng.* doi: 10.1186/2052-336X-12-79. Available from: <<http://www.ijehse.com/content/12/1/79>>.
- [46] M. El Haddad, A. Regti, R. Slimani, S. Lazar, Assessment of the biosorption kinetic and thermodynamic for the removal of safranin dye from aqueous solutions using calcined mussel shells, *J. Ind. Eng. Chem.* 20 (2014) 717–724.
- [47] R. Slimani, I. El Ouahabi, F. Abidi, M. El Haddad, A. Regti, M.R. Laamari, S.E. Antri, S. Lazar, Calcined eggshells as a new biosorbent to remove basic dye from aqueous solutions: Thermodynamics, kinetics, isotherms and error analysis, *J. Taiwan Inst. Chem. Eng.* 45 (2014) 1578–1587.
- [48] Y. Lin, S. Xu, J. Li, Fast and highly efficient tetracyclines removal from environmental waters by graphene oxide functionalized magnetic particles, *Chem. Eng. J.* 225 (2013) 679–685.
- [49] K. Li, F. Ji, Y. Liu, Z. Tong, X. Zhan, Z. Hu, Adsorption removal of tetracycline from aqueous solution by anaerobic granular sludge: Equilibrium and kinetic studies, *Water Sci. Technol.* 67 (2013) 1490–1496.
- [50] M. Islam, R.K. Patel, Evaluation of removal efficiency of fluoride from aqueous solution using quick lime, *J. Hazard. Mater.* 143 (2007) 303–310.
- [51] S. Lagergren, About the theory of so-called adsorption of soluble substances, *K. Sven. Vetenskapskad. Handl.* 24 (1898) 1–39.
- [52] G. Crini, H.N. Peindy, F. Gimbert, C. Robert, Removal of C.I. Basic Green 4 (Malachite Green) from aqueous solutions by adsorption using cyclodextrin-based adsorbent: Kinetic and equilibrium studies, *Sep. Purif. Technol.* 53 (2007) 97–110.
- [53] N. Gupta, A.K. Kushwaha, M.C. Chattopadhyaya, Adsorptive removal of Pb²⁺, Co²⁺ and Ni²⁺ by hydroxyapatite/chitosan composite from aqueous solution, *J. Taiwan Inst. Chem. Eng.* 43 (2012) 125–131.